Measurement of the anisotropy of the energy of an isotropic-smectic interface in a smectic cylinder: Application to the L_3-L_α interface

Christophe Blanc*
Laboratoire de Minéralogie-Cristallographie de Paris, CNRS UMR 7590, T16 case 115, Université Pierre et Marie Curie, 4 Place Jussieu, F-75252 Paris Cedex 05, France
(Received 30 January 2001; published 12 June 2001)

In order to measure the relative anisotropy of a smectic-isotropic interfacial energy, we propose an alternative to the classic Wulff construction. We derive the Gibbs-Thomson equation that describes the equilibrium of a droplet of isotropic phase in a smectic sample confined within a cylindrical capillary. We then discuss the influence of the curvature energy term and show that the profile of the droplet gives the variation of the surface energy, either analytically or by means of a modified Wulff construction. From this approach, we measure the relative anisotropy of the sponge-lamellar interfacial energy in the dilute Cetylpyridinium Chloride/hexanol/brine surfactant system. We quantitatively confirm and complete previous observations of this interface, which displays strong crystalline features, such as cusps and forbidden orientations.

DOI: 10.1103/PhysRevE.64.011702 PACS number(s): 61.30.Hn, 61.30.Jf, 68.05.Cf, 61.30.St

I. INTRODUCTION

One of the main parameters that controls the shape and the growth patterns of crystalline materials on a macroscopic scale is the dependence of the interfacial tension $\sigma(\theta,\varphi)$ on the orientations of the crystal defined by the spherical angles θ and φ. The equilibrium shape of rigid crystals in their melt is indeed determined by their surface energy function as Wulff [1] showed in a famous paper. The anisotropy of the interfacial tension also controls several important mechanisms concerning the nonequilibrium dynamics of interfaces such as the formation of stationary needle crystals (dendrites) [2,3], even if other parameters such as the kinetic anisotropy or the diffusion (matter and heat) anisotropy are also relevant. Therefore, the anisotropy of the interfacial tension has to be measured when studying the shape and patterns created by a growing crystal. The classical method for rigid crystals consists of studying the equilibrium shape of an isolated germ by means of the Wulff construction, which relates the equilibrium shape to the polar plot $\sigma(\theta,\varphi)$ [2] of the interfacial energy (see Fig. 1).

This method cannot be straightforwardly applied to soft matter crystals such as smectic, hexagonal phases in their melt [and also to two-dimensional (2D) phases of Langmuir monolayers], because these soft crystals are easily distorted in the bulk by surface effects. For example, the nuclei of a lamellar phase within its isotropic phase display bulk defects such as focal conic domains [4] or curvature walls [5], which spontaneously appear and decrease the total energy of the crystals, interfacial energy included. The curvature energy of a given texture varies as $K\mathcal{R}$ (where K is a curvature modulus and $\mathcal{R}$ is the size of the droplet), whereas the interfacial energy varies as $\sigma\mathcal{R}^2$. The surface terms of a crystal dominate the bulk elasticity in the limit of large sizes (larger than $\mathcal{R}_c \approx K/\sigma$) with the result that its equilibrium shape tends to become spherical even if the interfacial energy is strongly anisotropic [4,6]. Although different authors [7–10] have tried to generalize the Wulff construction of curved crystals by taking the elastic effects into account, only particular geometries have been considered. Incidentally, it should be noted that the experimental study of the shape of isolated and curved nuclei cannot generally provide the variation of the interfacial tension over a large range of orientations, because the appearance of curvature and defects precisely tends to favor the presence of a narrow range of orientations of lowest interfacial energy.

Therefore, in practice, the measurement of the anisotropy in the interfacial tension of a soft crystal requires the orientation of this crystal by external means. The most common technique is the study of confined nuclei in thin samples, oriented by means of a strong anchoring on a transparent substrate. This technique has been successfully employed to obtain the angular dependence of several interfacial tensions related to the discotic hexagonal-isotropic [11], the SmA-SmB [12], the hexagonal columnar-isotropic [13], and the nematic-SmB [14] interfaces. However, two main experimental difficulties limit the use of thin samples. First, a confined liquid crystal between two plane surfaces cannot be considered to be a 2D crystal because of the wetting conditions on the two limiting surfaces. This point has been studied in detail in Ref. [15], which shows that errors on the anisotropy could be as large as 25% when one does not take the presence of the meniscus into account. The second ex-

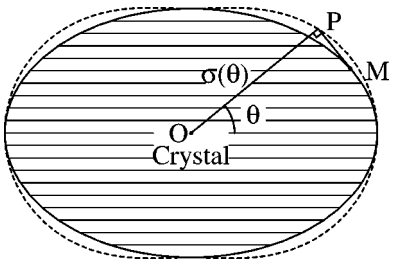

FIG. 1. A 2D Wulff construction applied to a lamellar rigid crystal (plain lines). The length OP gives the polar plot of the interfacial tension $\sigma(\theta)$ (dotted lines).

*Electronic address: blanc@lmcp.jussieu.fr

perimental difficulty concerns the achievement of a suitable anchoring—for example, a planar one is required for the study of a smectic-isotropic interface in thin samples. If such anchorings are usually well documented for thermotropic systems, it is not the case for lyotropic systems.

We have encountered this experimental difficulty when studying the two-phase region of surfactant systems, in which an isotropic L_3 sponge phase and a L_α lamellar phase coexist. The L_3 and L_α phases of membranes are found in the dilute part of the phase diagram of surfactant systems. The L_α phase is made of parallel bilayers of spacing d_α with a smectic order, whereas the isotropic L_3 phase consists in a disordered medium in which a single bilayer separates the solvent into two equivalent parts, with many connections, passages, and handles (the typical interbilayer distance is denoted d_3) [16].

In some surfactant systems [17,18] (see below), the nuclei of lamellar phases appear in the sponge phase as classic spherulites (onions) with L_α layers tangent to the interface. In other systems [19], the situation is very different. For example, previous studies [20–22] of the cetylpyridinium chloride (CPCl)/hexanol/brine surfactant system have reported the observations of very uncommon shapes and patterns obtained during the growth of the L_α phase in the isotropic L_3 phase. This result has suggested that strong crystalline interfacial effects (such as forbidden orientations and cusps [22]) were present even in the most dilute samples [23]. We therefore proposed that a preferred tilt angle θ_0 of the layers at the interface arises from a L_3-L_α epitaxy due to the continuity of the membranes through the interface and the matching of the typical distances d_3 and d_α [21]. We were, however, not able to obtain 2D equilibrium single crystals and to measure the anisotropy in the interfacial energy by means of one of the classic methods described above, because no method of planar alignment for the dilute lamellar phases is known. On the other hand, the studied lamellar phase is strongly *homeotropically* oriented by glass and we have reported the spontaneous formation of crystalline equilibrium droplets of L_3 phase [22] (see Fig. 2) within a smectic cylinder inside a cylindrical capillary. This geometry is known for orienting smectic layers in a leeklike way [24,25].

The present paper is dedicated to the study of the shape of a droplet of isotropic phase within a smectic cylinder (Sec. II) and of the angular dependence of its interfacial energy. We have thus obtained a quantitative measure of the anisotropy of the L_3-L_α interfacial energy in the CPCl system (Sec. III) and have explained several striking features of the textures and shapes in the two-phase region.

II. THE SHAPE OF AN INVERSE SMECTIC CRYSTAL IN A SMECTIC CYLINDER

Consider a droplet of isotropic phase within a smectic cylinder, in a meridian plane, as shown in Fig. 3. Because of the liquid character of the layers, the interface energy depends only on θ, the angle between the normal of the layers (the director), and the normal of the interface. The shape of the droplet can be described by $\rho(s)$ where s is the arc length

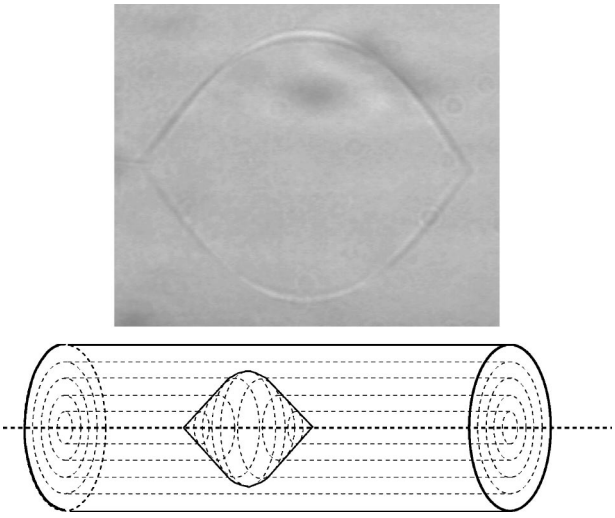

FIG. 2. Top: Droplet of isotropic L_3 phase within a stacking of cylindrical layers of L_α phase for the lyotropic system cetylpyridinium chloride (CPCl)/hexanol/brine (NaCl 1% wt. in water; wt. ratio hexanol over CPCl≈1.13; volume fraction of brine ≈ 0.92). Width of the picture 100 μm. Below: sketch of the geometrical arrangement of the layers in the capillary.

along a meridian and ρ the distance from the axis Δ. The Gibbs-Thomson (GT) equation of the interface (which relates the shape of the droplet to the interface and bulk free energies) can be obtained as follows. Consider a change in the shape due to a displacement $\delta h(s)$ along the normal of the interface (see Fig. 3).

Calling Δf the excess of free energy of the smectic phase compared to the isotropic phase and $f_e = K/2\rho^2$ the density of curvature energy of the lamellar layers, the change of shape corresponds to a bulk energy increase

$$\delta \mathcal{F}_\mathcal{V} = -\int 2\pi\rho(\Delta f + f_{el.})\,\delta h\,ds. \tag{1}$$

The normal displacement δh yields an increase in the elementary area from $2\pi\rho ds$ to $2\pi(\rho+\delta h\cos\theta)(1+\delta h/R)ds$

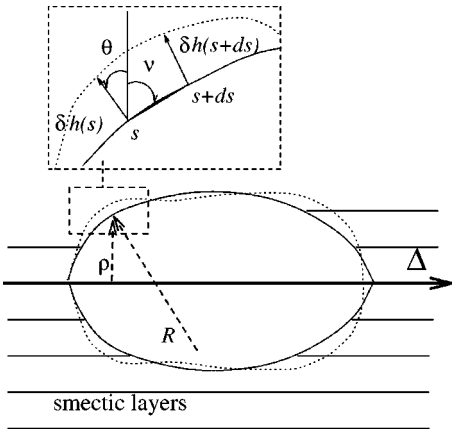

FIG. 3. The total free energy of an equilibrium droplet is stationary with regard to a small normal displacement δh of its shape.

where R is the local curvature radius of the meridian curve, but also a change $\delta\theta = d\,\delta h/ds$ in the orientation. Therefore the surface energy increase is

$$\delta\mathcal{F}_S = \int \sigma(\theta+\delta\theta)2\pi(\rho+\delta h\cos\theta)\left(1+\frac{\delta h}{R}\right)ds - \int 2\pi\sigma(\theta)\rho ds \approx 2\pi\int\left[\rho\left(\frac{\sigma\delta h}{R}+\frac{d\sigma}{d\theta}\frac{d\delta h}{ds}\right)+\sigma(\theta)\delta h\cos\theta\right]ds. \tag{2}$$

Performing integrations by parts and taking into account that $d\cdot/ds = -R^{-1}d\cdot/d\theta$ and $d\rho/ds = \sin\theta$, Eq. (2) leads to the first order in δh to

$$\delta\mathcal{F}_S = 2\pi\int ds\left\{\rho\left[\sigma(\theta)\frac{\delta h}{R}+\frac{\sigma''(\theta)}{R}\delta h\right]-\sin\theta\sigma'(\theta)\delta h + \sigma(\theta)\delta h\cos\theta\right\}. \tag{3}$$

The total free energy $\mathcal{F}_S+\mathcal{F}_V$ of an equilibrium crystal is stationary with regard to any normal displacement, which leads to the GT equation of the smectic-isotropic interface in a smectic-cylinder geometry:

$$\frac{\sigma(\theta)+\sigma''(\theta)}{R}+\frac{\sigma(\theta)\cos\theta-\sigma'(\theta)\sin\theta}{\rho} = -(\Delta f + f_{el.}). \tag{4}$$

This equation differs from the classic 2D GT equation for a crystal (which can be solved by the graphical construction of Fig. 1) [2]

$$\frac{\sigma(\theta)+\sigma''(\theta)}{R} = -\Delta f, \tag{5}$$

by the presence of two terms of different origins. The additional term on the left-hand side of Eq. (4) is due to the three-dimensional (3D) geometry; its scaling with length is the same as the first term. The curvature term $f_{el.} = K/2\rho^2$ scales differently, consequently, the equilibrium shapes are not size invariant. The left-hand side is of order $\sigma_0/\mathcal{R}$, where $\mathcal{R}$ is the typical size and typical curvature radius of the droplet and σ_0 the magnitude of the interfacial energy. To compare this term with $f_{el.}$, let us take $\sigma_0 \approx kT/d^2$ and $K \approx kT/d$ where d is a microscopic distance (e.g., the typical thickness of the smectic layers [26]). The curvature energy in Eq. (4) is negligible when $\rho \gg \rho_a = \sqrt{\mathcal{R}d}$. For a typical droplet of size 100 μm and $d \approx 1$–10 nm, $\rho_a \leqslant 1$ μm, which means that, on a macroscopic scale, the curvature energy does not distort the shape of the isotropic droplet, except for a very thin region surrounding the axis. To study more precisely the effect of the elastic energy on the shape, consider now the case of an isotropic tension $[\sigma(\theta)=\sigma_0]$. The total free energy of a droplet is then given by

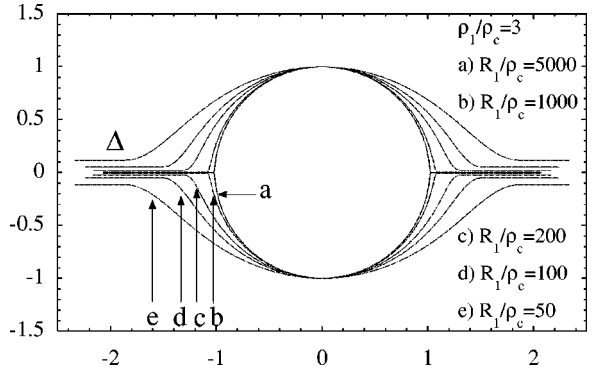

FIG. 4. Effects of the lamellar elasticity on the shapes of an isotropic inclusion within a smectic cylinder (the interfacial energy is isotropic).

$$\mathcal{F} = \int 2\pi\sigma_0\frac{d\rho}{\sin\theta} - \int \pi\rho^2\Delta f\frac{d\rho}{\tan\theta} - \int K\pi\ln\frac{\rho}{\rho_c}\frac{d\rho}{\tan\theta}, \tag{6}$$

where $\rho_c \approx d$ is a cutoff length along the axis for the curvature energy. Minimizing $\mathcal{F}$ with respect to $\theta(\rho)$ yields

$$\cos\theta = \frac{\rho}{R_0}+\frac{\rho_1}{\rho}\ln\frac{\rho}{\rho_c}, \tag{7}$$

where $R_0 = 2\sigma_0/\Delta f$ and $\rho_1 \approx K/2\sigma_0 \approx d$. Calling R_1 the largest radius of the droplet and scaling all lengths by R_1, Eq. (7) becomes

$$\cos\theta = \tilde{\rho}+\frac{\tilde{\rho}_1}{\tilde{\rho}}\ln\frac{\tilde{\rho}}{\tilde{\rho}_c}+\tilde{\rho}_1\tilde{\rho}\ln\tilde{\rho}_c. \tag{8}$$

Figure 4 shows the evolution of the shape obtained from Eq. (8) for different ratios R_1/ρ_c and $\rho_1/\rho_c = 3$. When the size of the droplet becomes much larger than ρ_c, the elastic effects along the core do not modify the overall shape. In passing, it should also be noted that by taking ρ_1 larger than a few times ρ_c, one finds a stable core of isotropic phase along the axis of the smectic cylinder, far from the droplet. Such a mechanism could be an efficient way to relax the curvature of the core of a smectic cylinder close to an isotropic phase and could be an alternative to the appearance of the mechanical instability of smectic cylinders discussed in Ref. [25].

In conclusion, the curvature energy present in the smectic cylinder modifies the shape of the smallest crystals but not of large ones. When the order of the ratio R_1/ρ_c is much larger than 1000 (a typical value), the curvature energy of the smectic layers does not contribute significantly to the shape of the inverse smectic crystals.

When the curvature energy can be neglected in Eq. (4) (that is for not too small droplets), it is straightforward to check that $\sigma(\theta)\cos(\theta)-\sigma'(\theta)\sin(\theta) = A\rho$ with $A = \Delta f/2$ fulfills Eq. (4), which then reduces to

$$\frac{\sigma(\theta)+\sigma''(\theta)}{R} = -\Delta f/2. \tag{9}$$

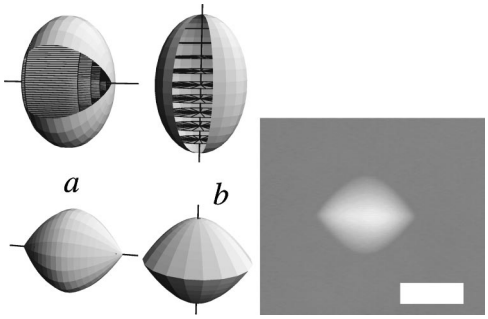

FIG. 5. The equilibrium shape [(a)-top] of an arbitrary isotropic droplet in a cylindrical arrangement of smectic layers has the same 2D profile than the equilibrium shape of its rigid crystal [(b)-top] but a different 3D shape (some smectic layers have been sketched inside both droplets). This phenomenon is observed [(a),(b)-bottom] in dilute samples of the CPCl system where the corresponding shapes are given in Fig. 2 and in the micrograph of the right picture, which shows a L_α nuclei made of planar layers (Brine volume fraction 0.92; bar 20 μm. Crossed polarizers at 45° of vertical).

Equation (9) has the form of a classic 2D GT equation [Eq. (5)]. It means that the contour of a droplet is similar to the shape of a true 2D rigid crystal and that the anisotropy of interfacial energy can be obtained from a classic Wulff construction.

Note, however, that the 3D shape of a smectic cylinder droplet is different from the usual 3D Wulff construction shape (which can be also built from the 2D Wulff construction by rotating the 2D crystal shape around the director axis). In a smectic cylinder, the axis of revolution of the shape is indeed the cylinder axis and not the smectic director. We have sketched the two shapes of an arbitrary droplet corresponding to a cylinder smectic and to planar layers in Fig. 5. This difference can be observed in dilute samples of CPCl system for which the anisotropy in the interface energy is not too large (see Sec. III) and where small direct L_α crystals can be observed. A droplet, shown in Fig. 5, displays a profile similar to the contour of the smectic cylinder droplet of Fig. 2, but the 3D shapes do not have the same axis of revolution.

III. APPLICATION TO THE L_3-L_α INTERFACIAL ENERGY

Applying the results of Sec. II, we have systematically measured the anisotropy of interfacial tension of the L_3-L_α interface of the cetylpyridinium chloride/hexanol/brine surfactant system.

A. Experiment

The chemical components (cetylpyridinium chloride and hexanol from Aldrich) have been mixed with brine (1% wt. of NaCl in water) and held at rest several days before use. The samples have been either prepared in the L_α-L_3 two-phase region at room temperature (for a weight ratio hexanol over CPCl h/c between 1.05 and 1.11) or within the close L_3 phase at different volume fractions of solvent ϕ_w comprised between 0.73 and 0.92.

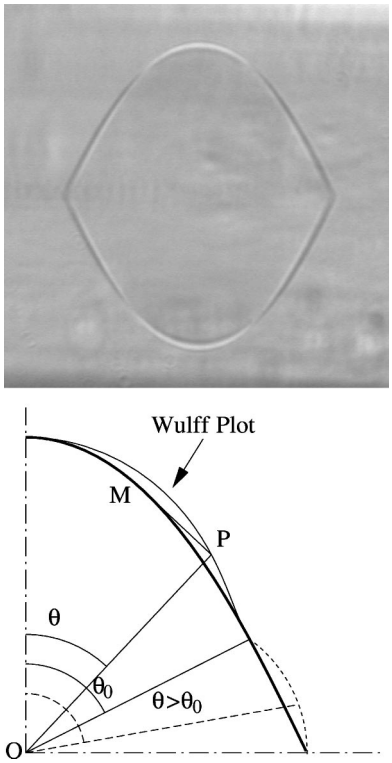

FIG. 6. Top: Contour of a L_3 droplet within the L_α smectic cylinder at a brine volume fraction $\phi_w = 0.82$ (picture width: 200 μm). Bottom: corresponding Wulff plot of the upper-right part of the shape.

Clean cylindrical glass capillaries (diameter 300 μm) are filled, flame sealed, and observed under polarizing microscope (Leitz DMRXP) equipped with a hot stage (Mettler 82HT) and a movie camera. Heating the sample yields [28] an increase of the amount of lamellar phase at the expense of the sponge phase. Since the two-phase region is quite large in temperature (about 20 °C for a brine volume fraction $\phi_w = 0.75$), very stable droplets of isotropic L_3 phase can be isolated within the lamellar phase. This latter is spontaneously oriented by the glass capillary in a leeklike way, in a few hours. The quality of the alignment of the lamellar phase is then checked under the polarizing microscope. During the same time, the droplets of L_3 phase along the cylindrical axis are stabilized with shapes independent of their size (typical diameter $100-200$ μm) and of their history. When the samples are prepared in the two-phase region close to the lamellar phase at room temperature (that is with a very few amount of sponge phase and $h/c \approx 1.05$) such droplets can be kept for several days without any change of shape. We apply then the Wulff construction (Fig. 6) in order to obtain the angular dependence $\sigma(\theta)$.

B. Results and discussion

The shapes of the droplets do not depend on the temperature (for a given dilution) but change with dilution as shown in Fig. 7. The droplets display conical facets, corresponding to one particular orientation θ_0 (with the notation of Figs. 3 and 6), and two singularity points. Orientations comprised

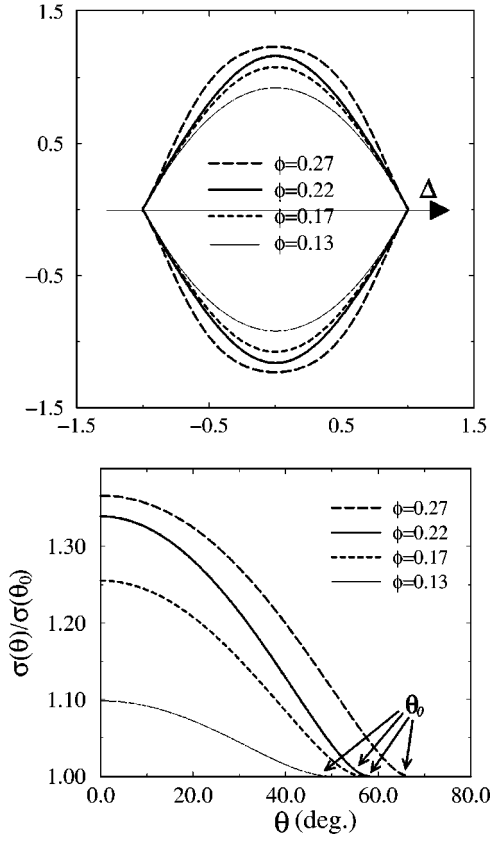

FIG. 7. Top: Evolution of the shape of the droplets with the membrane volume fraction $\phi = 1 - \phi_w$. Bottom: Relative anisotropy of the interfacial tension $\sigma(0)/\sigma(\theta_0)$ obtained from their Wulff construction.

between θ_0 and $\pi/2$ are not present in the equilibrium shapes. We give the relative interfacial tension $\sigma(\theta)/\sigma(\theta_0)$ of the corresponding shapes in Fig. 7; note that θ_0 smoothly increases with the membrane volume fraction from 45° to 70° for $\phi \approx 0.3$. The interfacial energy decreases with increasing tilt angle up to the largest observed orientation, which coincides with θ_0 (defined with an accuracy of $\pm 1°$). The anisotropy in the interfacial energy, that we will explicitly define as the ratio $\sigma(0)/\sigma(\theta_0)$, decreases with the brine volume fraction but remains quite large (around 10% for $\phi_w = 0.87$).

Is the orientation θ_0 a facet, or simply a strong minimum for the interfacial energy? The Wulff plot does not give the interface tension for orientations larger than θ_0 because these orientations do not appear in the equilibrium shapes (such orientations are called forbidden [30]). However, we can easily obtain a lower limit for the interfacial energy in that region. Consider indeed the sketch in Fig. 6. The fact that the orientations $\theta > \theta_0$ are forbidden indicates that the corresponding interfacial energy [27] is located above the dotted curve (if it were lower, such orientations would indeed appear in the equilibrium shapes). More precisely, the geometric construction defines the lower limit for the interfacial energy $\sigma_f(\theta) = \sigma(\theta_0)\sin\theta/\sin\theta_0$ [this latter result satisfies the usual *local* stability criterion [2] of an interface $\sigma(\theta) + \sigma''(\theta) > 0$].

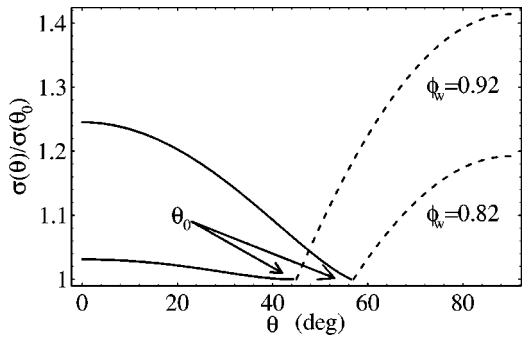

FIG. 8. Relative interfacial tension ($\theta < \theta_0$) and its lower limit ($\theta > \theta_0$) for two brine volume fractions $\phi_w = 0.82$ and $\phi_w = 0.92$ of the CPCl system. The orientation θ_0 is a cusp for the interfacial energy.

The Wulff plot completed in that way in Fig. 8 shows the presence of a cusp at the angle θ_0. This last result strongly reinforces the notion of epitaxy at the L_3-L_α interface [21,23]. The existence of a cusp at θ_0 was indeed predicted by Lavrentovich *et al.* (Ref. [23]) who developed a model based on the appearance of Frankel-Kontorowa dislocations when the orientation slightly departs from θ_0. However this model also predicted the existence of a *symmetric* cusp. Therefore, our results suggest that mechanisms other than dislocations are involved when the orientation is not exactly θ_0. A more complete model explaining all the features described previously, especially the forbidden orientations and the asymmetric cusp, remains to be developed.

C. Bulk faceting *vs.* Herring instability

During the L_α phase free growth [20,21], the tilt angle θ_0 is observed over the main part of the interface. Depending on the global orientation of the interface, two different mechanisms participate in that phenomenon.

First, forbidden orientations are thermodynamically unstable [30] on a local scale and therefore should never be observed. It is consistent with our observations; *any* such interfaces in L_α nuclei or domains indeed consist in hill-and-valley interfaces, as shown in Fig. 9. The Herring's instabil-

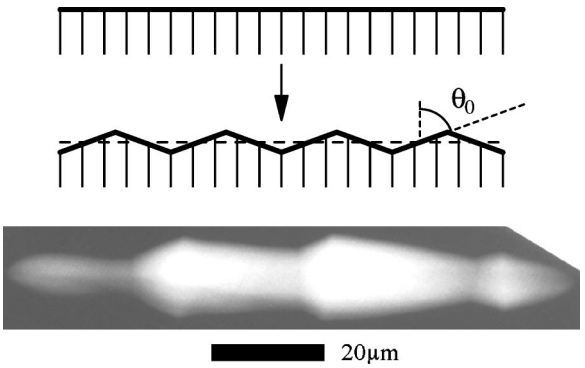

FIG. 9. Top: A global orientation of interface perpendicular to the layers is forbidden and is unstable with respect to the formation of an hill-and-valley instability (as in the nucleus shown in bottom picture).

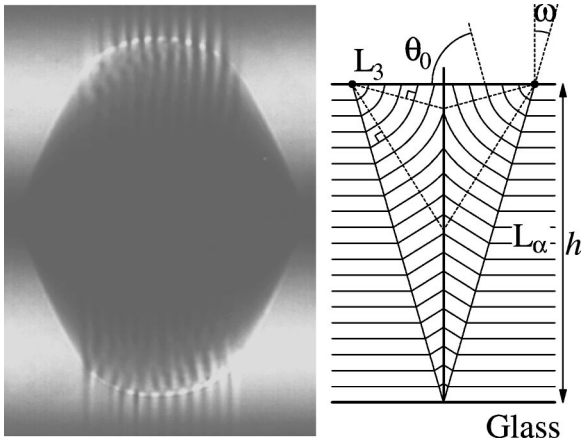

FIG. 10. Perfect droplets of isotropic phase within the smectic cylinder have not been obtained in the concentrate part of the CPCl surfactant system. Networks of defects (sketched in right picture) appear at locations where the orientation at the interface is much different from θ_0. View between crossed polarizers at 45° from vertical. Brine volume fraction 68%.

ity is responsible for the appearance of the ''crystalline'' shapes of L_α nuclei, which are observed even in the most dilute samples.

On the other hand, the softness of the L_α phase also contributes to the faceting of the droplets in a much different way. For example, the study of inverse droplets has not been extended below $\phi_w = 75\%$ because droplets of L_3 phase within a perfect cylinder lamellar phase were not obtained at such concentrations. An interface of orientation $\theta < \theta_0$ is indeed unstable towards bulk faceting (the formation of bulk defects due to interfacial effects at a smectic-to-isotropic interface). This effect is observed in concentrated solutions as shown in Fig. 10. Because of the large anisotropy of the interfacial tension, the tangential orientation is no more stable and focal conic domains appear in order to ensure the orientation θ_0 almost everywhere on the surface of the droplet. This phenomenon has been studied in detail for thin slabs in Ref. [5,29], where we have shown that the energy of a single defect was given (in units of $\alpha^2 \pi K \lambda$) by

$$E(x,\omega) = -\Phi x^2 \omega^2 + x\omega + \frac{2}{3} x^2 \omega^4, \tag{10}$$

where $\Phi = \Delta\sigma\lambda/K$, $x = h/\alpha\lambda$ is the dimensionless thickness of the lamellar slab, α is a numerical factor ≈ 30, $\Delta\sigma = \sigma(0) - \sigma(\theta_0)$, K the bulk curvature modulus, and λ the smectic penetration length. The typical thickness h_c for which the defects appear is given by [29]

$$E(x,\omega) = 0$$

$$\frac{\partial E}{\partial \omega} = 0, \tag{11}$$

which yields

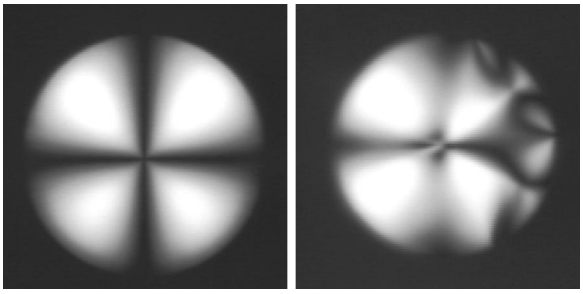

FIG. 11. The L_α nuclei of the SDS system appear in the L_3 sponge phase as spherulites (left). However, the textures get rapidly reorganized in a few minutes by means of focal conic domains (right). Crossed polarizers; width of the pictures 80μm.

$$h_c = \frac{3\alpha\lambda}{\sqrt{2}\Phi^{3/2}}. \tag{12}$$

In a lamellar phase stabilized by Helfrich's steric interaction [31], we expect that $\lambda = 8\kappa\delta/3\pi kT\phi$, where δ is the membrane thickness and $\kappa \approx Kd \approx kT$ is the bending modulus of the membrane. The term Φ can therefore be written as

$$\Phi = \frac{\Delta\sigma}{\sigma(\theta_0)} \frac{\sigma(\theta_0)\lambda}{K}. \tag{13}$$

We expect that the $\sigma(\theta_0)$ varies as $\sigma(\theta_0) \approx \sin^2\theta_0 \phi^2 \kappa/\delta^2$ [23]. The threshold therefore varies as

$$h_c \approx \frac{3\alpha\lambda}{\sqrt{2}\Phi^{3/2}}$$

$$\sim \frac{1}{\phi\left(\frac{\Delta\sigma}{\sigma(\theta_0)}\right)^{3/2}}. \tag{14}$$

Both ϕ and $\Delta\sigma/\sigma(\theta_0)$ increase with the membrane volume fraction, which means that the largest possible thickness of perfect lamellar slab in contact with the droplet decreases. Around $\phi_w \approx 70\%$, the measured threshold is $h_c \approx 30$–40 μm [5]. Droplets with a L_α slab larger than this value h_c for the tangential orientation are therefore unstable towards bulk faceting.

Eventually, we have also observed another lyotropic system, for which the lamellar phase appears in the sponge phase as spherulites. As observed by Buchanan *et al.* [18] in the sodium dodecylsulfate (SDS)/octanol/brine system, such spherulites do not consist of perfect spherical layers but display focal conic domains. We have observed samples—weight ratio octanol/SDS ≈ 1.36, brine (20 g NaCl/l) volume fraction $\phi_w = 70\%$—cooled from the sponge phase ($T = 40°$) into the two-phase region ($T = 25°$). Lamellar nuclei appear as perfect onions but when their size increases (and/or with time), numerous defects destroy the bulk lamellar arrangement or even reorganize the whole texture as shown in Fig. 11.

We propose the following scenario to explain the appearance of such droplets. The anisotropy in the interfacial energy of this system is quite weak but favors the angle θ_0 (we have measured $\sigma(0)/\sigma(\theta_0) \approx 1.05-1.1$ and $\theta_0 \approx 60°$ at $\phi_w = 0.7$). Spherulites can nevertheless be spontaneously created during the growth (because, for instance, of the nucleation of the first layers around nearly spherical impurities). Contrary to the CPCl system, the anisotropy of interfacial tension is too weak to destabilize easily the interface and the growth is isotropic, which keeps the shape spherical. However, when the size of the droplets reaches a critical size, close to the critical thickness of thin planar samples, the bulk faceting yields an assembly of focal conic domains around the sphere. Note also that it means that the presence of onions in a biphasic solution does not necessarily indicate that the interface is of minimal energy when the layers are parallel to it.

IV. CONCLUDING REMARKS

We have measured the angular dependence of the L_3-L_α interface in the CPCl/brine/hexanol surfactant system. We have unambiguously shown that a cusp in the interfacial energy was present for an orientation θ_0 corresponding to the lowest interfacial energy. The presence of forbidden orientations ($\theta > \theta_0$) is the source of an hill-and-valley instability (as reported in Ref. [20] about free-growth shapes). Therefore the two types of faceting occurring in the L_α-L_3 two-phase region have two different origins. The first one (the Herring's instability) is local and arises when the global orientation of the interface is a forbidden orientation. The second one (bulk faceting) arises when the global orientation of the interface is not forbidden but is of large energy. These instabilities are both present in the nuclei of L_α phase in sponge phase and play the same role, that is, they impose the same orientation θ_0 all over the interface. Note however that the Herring's instability has a local origin and is therefore present at each scale, whereas bulk faceting implies a competition between bulk deformation and surface effects and thus occurs only at large scale (that is in large L_α domains).

Note finally that the shapes of droplets of lamellar phase do not depend only on the equilibrium properties of the interface but also on the specific properties of the growth mechanisms. The two types of faceting play different roles during the L_α phase growth. The Herring's instability is expected to be present at any rate of growth (at least when the interface is in local equilibrium, which is almost always assumed in free growth experiments), whereas bulk faceting requires deformations of matter and involves hydrodynamic modes. The importance of each instability is therefore expected to be very different according to the growth rate of the lamellar phase [32].

In this paper, we have also shown that a modified Wulff plot can be used to measure the anisotropy of an interfacial energy from the shape of a droplet of isotropic phase within a smectic cylinder. If the method we have developed can be considered as an alternative of the classic Wulff construction when studying a smectic-to-isotropic interface, it is however limited for two reasons. First, when the elastic effects cannot be neglected, the graphical construction should be replaced by the numerical integration of Eq. (4). Moreover when the anisotropy of interfacial tension is important, bulk faceting is expected, even in the presence of a strong anchoring at the substrate.

ACKNOWLEDGMENTS

The author would like to thank Dr. M. Kleman for critical reading of the manuscript.

[1] G. Wulff, Z. Kristallogr. Mineral. **34**, 449 (1901); see also L. Landau and E. Lifshitz, *Statistical Physics* (MIR, Moscow, 1967).
[2] See, for example, C. Godrèche, *Solids Far From Equilibrium* (Cambridge University press, Cambridge, 1992).
[3] P. Pelcé, *Dynamics of Curved Fronts* (Academic Press, Boston, 1988).
[4] J.B. Fournier and G. Durand, J. Phys. II **1**, 845 (1991).
[5] C. Blanc and M. Kleman, Eur. Phys. J. B **10**, 53 (1999).
[6] C. Blanc and M. Kleman, Eur. Phys. J. E **4**, 241 (2001).
[7] J.B. Fournier, Phys. Rev. Lett. **75**, 854 (1995).
[8] P. Galatola and J.B. Fournier, Phys. Rev. Lett. **75**, 3297 (1995).
[9] J. Rudnick and R. Bruinsma, Phys. Rev. Lett. **74**, 2491 (1995).
[10] K.K. Loh and J. Rudnick, Phys. Rev. E **62**, 2416 (2000).
[11] P. Oswald, J. Phys. (France) **49**, 1083 (1988).
[12] P. Oswald, F. Melo, and C. Germain, J. Phys. (France) **50**, 3527 (1989).
[13] L. Sallen, P. Oswald, J.C. Géminard, and J. Malthête, J. Phys. II **5**, 937 (1995).
[14] A. Buka, T. TothKatona, and L. Kramer, Phys. Rev. E **49**, 5271 (1994).
[15] J.C. Géminard and P. Oswald, Phys. Rev. E **55**, 4442 (1997).
[16] See, for example, the review paper, G. Porte, J. Phys.: Condens. Matter **4**, 8649 (1992).
[17] In AOT/water/NaCl mixtures, as reported in, D.A. Antelmi, P. Kékicheff, and P. Richetti, Langmuir **15**, 7774 (1999).
[18] In SDS/brine/octanol mixtures, as reported in, M. Buchanan, L. Starrs, S.U. Egelhaaf, and M.E. Cates, Phys. Rev. E **62**, 6895 (2000).
[19] C. Blanc, Ph.D. thesis, University Paris VI, 2000 (unpublished).
[20] C. Quilliet *et al.*, C. R. Acad. Sci. Paris II **319**, 1469 (1994).
[21] C. Quilliet, C. Blanc, and M. Kleman, Phys. Rev. Lett. **77**, 522 (1996).
[22] C. Blanc and M. Kleman, Mol. Cryst. Liq. Cryst. **332**, 585 (1999).
[23] O.D. Lavrentovich, C. Quilliet, and M. Kleman, J. Phys. Chem. B **101**, 420 (1997).
[24] P. Bassereau, J. Marignan, and G. Porte, J. Phys. (Paris) **48**, 673 (1987).

[25] The smectic cylinders were originally studied in thermotropic systems, see P.E. Cladis, Philos. Mag. **24**, 641 (1974).

[26] These order of magnitude are particularly relevant for the diluted lyotropic lamellar phase since the curvature modulus is given by κ/d and the interfacial energy is expected to be of order κ/d^2 as shown in Ref. [23], where the bilayer curvature modulus κ is of order kT and d is the layer thickness.

[27] However, it should be noted that the interfacial tension above θ_0 is somewhat fictitious since the corresponding orientations cannot be observed. See a comment from a microscopic point of view in C. Rottman and M. Wortis, Phys. Rep. **103**, 59 (1984).

[28] Y. Nastishin, E. Lambert, and P. Boltenhagen, C. R. Acad. Sci. II **321**, 205 (1995).

[29] C. Blanc and M. Kleman, Phys. Rev. E **62**, 6739 (2000).

[30] C. Herring, Phys. Rev. **82**, 87 (1951).

[31] W. Helfrich, Z. Naturforsch. A **33**, 305 (1978).

[32] A more detailed study of the growth mechanisms of the L_α nuclei is in preparation.